J Mater Sci (2007) 42:6549–6554
DOI 10.1007/s10853-007-1514-0

Composition dependence of thermally induced second-harmonic generation in chalcohalide glasses

Haitao Guo · Xiaolin Zheng · Xiujian Zhao · Guojun Gao · Yueqiu Gong · Shaoxuan Gu

Received: 12 August 2006 / Accepted: 12 January 2007 / Published online: 30 April 2007

Abstract By investigating the second-harmonic generation (SHG) of the series $(100 - 2x)GeS_2 \cdot xGa_2S_3 \cdot xPbI_2$ (x = 5, 10, 15, and 20) chalcohalide glass samples after thermal poling, it was found that there was an optimal poling temperature for each composition and there was also a relation between optimal poling temperature and glass transition temperature. With increasing x, the obtained second-order susceptibility $\chi^{(2)}$ shows an increase first and then decrease, and the maximum was seen at x = 15. A dipole reorientation model and structural relaxation causing by Ga_2S_3 and PbI_2 were proposed to explain the dependence of poling temperature on SH intensity for each composition and the presence of the maximum $\chi^{(2)}$ in this chalcohalide glass series.

Introduction

Non-linear optical properties of transparent glasses are presently the focus of growing interest for elaboration of all-optical devices, such as photonic modulators, optical data storage and telecommunication, or for the spectral extension of laser sources. The researched glasses are mostly oxide glasses in previous studies, including fused silica [1, 2], tellurate glasses [3], Ti or Pb containing silicate glasses [4, 5] and microcrystal doped glasses [6], etc. On the other hand, various methods or techniques of poling have been successfully used to induce SHG in glasses, such as thermal poling, electron beam irradiation, UV light poling, proton implantation, corona discharge-assisted poling, and so on.

For chalcogenide and chalcohalide glasses, large SHG efficiencies are expected to occur due to large amount of defects and many high energy lone pair electrons in them. In 2000 and 2001, Liu et al. [7, 8] and Qiu et al. [9] reported their observations of SHG in the Ge–As–S chalcogenide glass by means of electron beam irradiation and all-optical poling, respectively. Recently, Guignard et al. [10, 11] observed SHG in the Ge–Ga–Sb–S and Ge–Sb–S chalcogenide glass by thermal poling and a second-order susceptibility $\chi^{(2)}$ of (8.0 ± 0.5)pm/V was obtained when $Ge_{25}Sb_{10}S_{65}$ glass was poled at 170 °C under (4.0–5.0) kV for 30 min. However, compared to oxide glasses mentioned above, the study of compositional effect on SHG in chalcogenide and/or chalcohalide glasses systems are few and the mechanism is not very clear yet. To our knowledge, only Nakane et al. [12] researched the SHG in the thermally poled GeS_x (x = 3, 4, 5, 6) glasses in 2005. In their report, the SH intensity depended on the S content and the origin of SHG is ascribed to the recombination of defects and relaxation of structural deformation after poling.

In this paper, an investigation of the second-order optical properties of a new series $(100 - 2x)GeS_2 \cdot x$-$Ga_2S_3 \cdot xPbI_2$ (x = 5, 10, 15, 20) chalcohalide glasses is reported. Based on the detailed poling analysis, interrelationships between the glass composition and poling temperature and the second-order non-linear optical properties were presented. Our work was aimed at the elucidation of the mechanism of the SHG in this novel chalcohalide glass

H. Guo (✉) · X. Zheng · X. Zhao · G. Gao · Y. Gong · S. Gu
Key Laboratory of Silicate Materials Science and Engineering, Ministry of Education, Wuhan University of Technology, Wuhan, Hubei 430070, P.R. China
e-mail: guoht_001@163.com

X. Zhao
e-mail: zhaoxj@public.wh.hb.cn

and a search of new material for non-linear optical devices in the future.

Experimental procedure

Sample preparation

The compositions of the studied glasses are $(100 - 2x)GeS_2{\cdot}xGa_2S_3{\cdot}xPbI_2$ with x = 5, 10, 15 and 20, while x is the mole percent. The bulk glasses were prepared by conventional melt-quenching technique using high-purity raw materials (5 N for Ge, Ga and S, 3 N for PbI_2). Details of the preparations were similar to the procedure in our previous work [13]. The $10 \times 10 \times 0.6$ mm^3 plate-like samples were prepared from the bulk glasses and polished to mirror smoothness on both sides.

Thermal poling process was carried out as follows. The glass sample was sandwiched between two commercial borosilicate glass plates (0.15 mm in thickness) and then contacted physically with cupreous electrodes. The glass sample sandwiched with the electrodes was put into a vessel filled with ethyl silicone oil and heated by electric furnace until to an aimed temperature (≤ 310 °C, below the boiling point of ethyl silicone oil). After held at the temperature for 30 min, an electric field 6.0 kV was applied for 40 min. Then the sample was removed from the furnace and cooled down to room temperature with the constant voltage still applied. It is apparent that the actual voltage applied to the glass sample was less than the displayed voltage because of the existence of the two commercial borosilicate glass plates.

Measurements

Visible–near IR transmission spectra of the samples were recorded between 400 nm and 1,100 nm by a spectrometer (Shimadzu UV-1601). Refractive indices between 300 nm to 1,300 nm were measured by using a Spectro-Ellipsometer (Woollam W-VASE). The glass transition temperature, T_g, was determined by the slope intercept method from curves obtained by using differential scanning calorimetry-thermogravimetry (DSC-TG) (Netzsch STA 449C) at a heating rate of 10 °C/min with a precision of ±1 °C. The SHG of the poled samples were measured in our laboratory by the Maker fringe device (Fig. 1) just like Dong et al. [14] did. The fundamental wave of a pulsed Nd:YAG laser with a pulse width of ~10 ns was used as the incident light.

Results

Figure 2 shows transmission spectrum in the visible–near IR of the $90GeS_2{\cdot}5Ga_2S_3{\cdot}5PbI_2$ glass with a 0.6 mm thickness. And at the operating wavelength (1,064 nm) and its SH wavelength (532 nm), the transmissions are about 81% and 54%, respectively. The refractive index of the investigated glass collected as a function of wavelength from 300 nm to 1300 nm is also shown in Fig. 2. It follows as typical dispersion curves of chalcohalide glasses. The refractive indices of these glasses are relatively high, which are rather beneficial to the enhancement of optical non-linear susceptibility and the application in optoelectronic field.

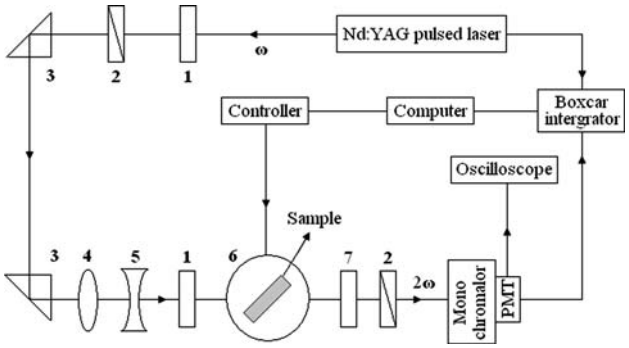

Fig. 1 Schematic illustration of the equipment for SHG measurement: (1) Vis cut filter; (2) polarizer; (3) Glan prism; (4) convex lens; (5) concave lens; (6) rotation stage; (7) IR cut filter

SHG was observed in the thermally poled $(100 - 2x)GeS_2{\cdot}xGa_2S_3{\cdot}xPbI_2$ (x = 5, 10, 15 and 20) glasses in our experiments. Figure 3 shows characteristic Maker fringe patterns of $80GeS_2{\cdot}10Ga_2S_3{\cdot}10PbI_2$ glass poled at 290 °C under 6.0 kV for 40 min and $70GeS_2{\cdot}15Ga_2S_3{\cdot}15PbI_2$ glass poled at 250 °C under 6.0 kV for 40 min. Maximum of SH intensity were obtained when the angles of incidence are ±60°.

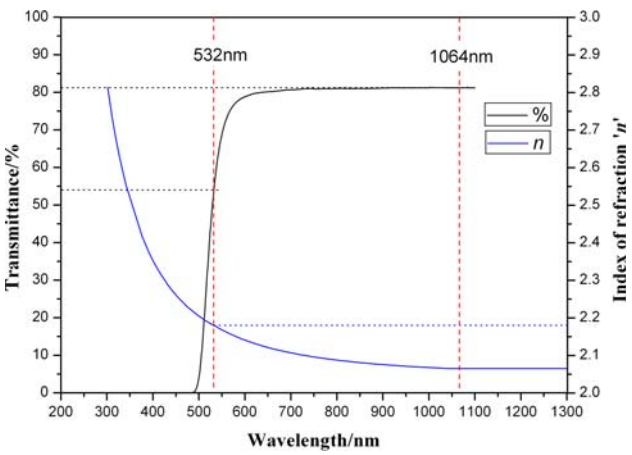

Fig. 2 Optical transmission and refractive indices of $90GeS_2{\cdot}5Ga_2S_3{\cdot}5PbI_2$ glass in UV–vis–NIR region

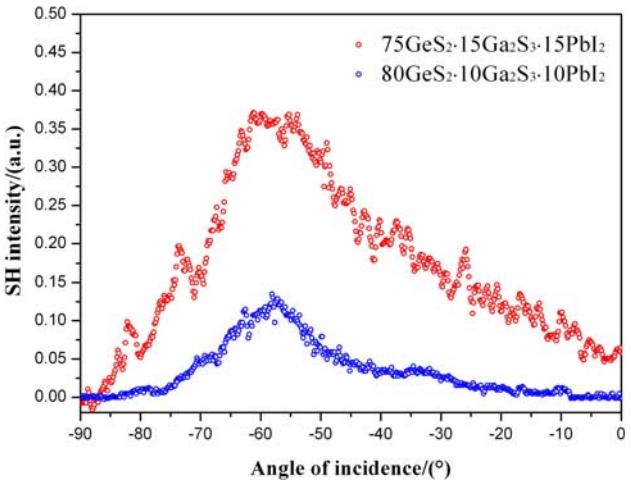

Fig. 3 Maker fringe patterns of $80GeS_2{\cdot}10Ga_2S_3{\cdot}10PbI_2$ (poled at 290 °C under 6.0 kV for 40 min) and $70GeS_2{\cdot}15Ga_2S_3{\cdot}15PbI_2$ (poled at 250 °C under 6.0 kV for 40 min) glasses

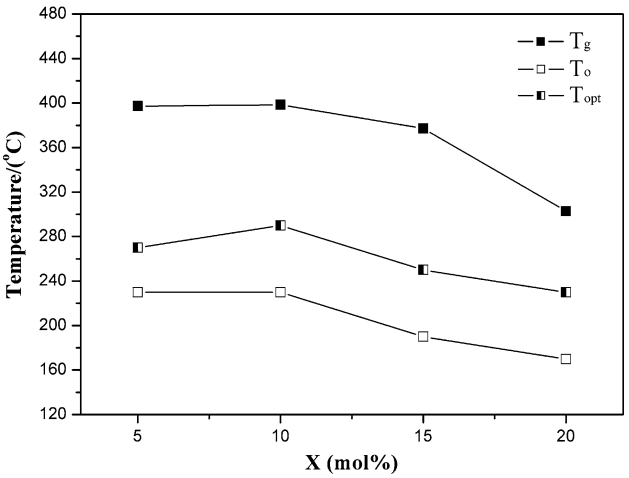

Fig. 5 Variation of the minimum poling temperature T_o at which SHG can be detected, optimal poling temperature T_{opt} and glass transition temperature T_g with mole percent x

Figure 4 shows the dependence of SH intensity on the poling temperature of four compositions. For each composition, SH signal was not detected below T_o, and once when the poling temperature was higher than T_o, increase of temperature will lead to larger SHG. We also found that the SH intensity can get a maximal value at the optimal poling temperature T_{opt} for each composition and when temperature was higher than T_{opt}, SH intensity gradually decreased.

Figure 5 depicts the relation between T_o, T_{opt} and T_g of each composition. There exists a relatively constant relationship between T_g and T_o, T_{opt}. That is, $T_g - T_o \approx 150$ °C and $T_g - T_{opt} \approx 100$ °C.

Under the condition of their own optimal poling temperature, a curve between SHG and mole percent x can be got as shown in Fig. 6. The SH intensity drastically increases with increasing Ga_2S_3 and PbI_2 contents from $x = 5$ to 15 in $(100 - 2x)GeS_2{\cdot}xGa_2S_3{\cdot}xPbI_2$ series, and then decreased at $x = 20$. Thus, there is a maximum at $x = 15$. Based on above study, a maximum second-order susceptibility $\chi^{(2)}$, 4 pm/V, was obtained when the $70GeS_2{\cdot}15Ga_2S_3{\cdot}15PbI_2$ glass was poled at 250 °C under 6.0 kV for 40 min.

Table 1 summarizes the values of the refractive indices at 1,064 and 532 nm (n_ω and $n_{2\omega}$), the corresponding coherence length $l_c (l_c = \lambda/[4(n_{2\omega} - n_\omega)])$, glass transition temperature T_g, minimum poling temperature T_o at which SHG can be detected, optimal poling temperature T_{opt}, maximum second-order susceptibility $\chi^{(2)}$ and mole percent x.

In order to determine the situation of non-linear layer of the poled samples, we also measured SHG of the glass samples after the anode-side surface was etched by

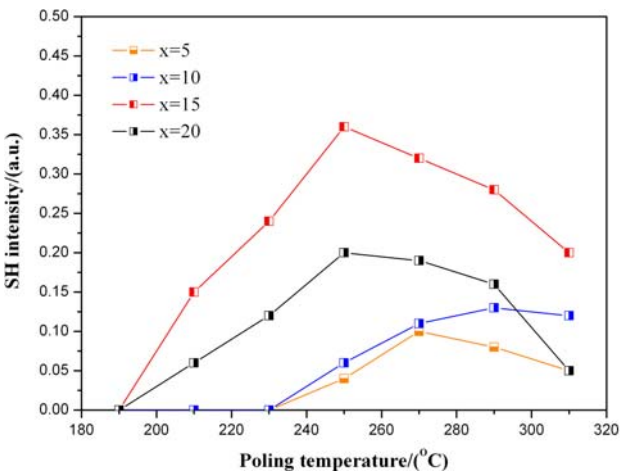

Fig. 4 Variation of the SH intensity with poling temperature for different four compositions

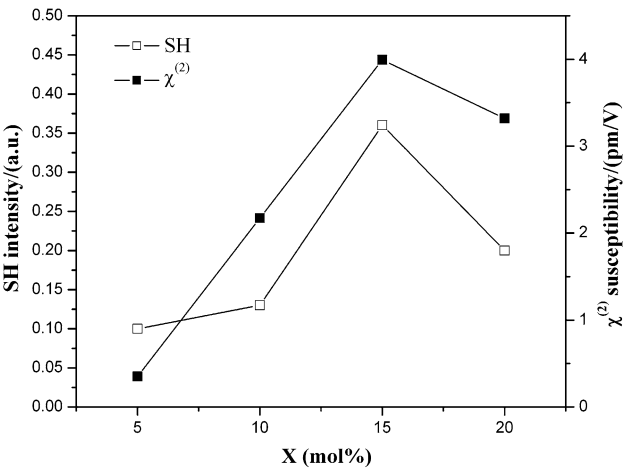

Fig. 6 Variation of the SH intensity and second-order susceptibility $\chi^{(2)}$ with mole percent x

Table 1 Compositions and properties of GeS_2–Ga_2S_3–PbI_2 system glasses

Composition (in mol%)	T_g [a] (°C)	T_o (°C)	T_{opt} (°C)	n_ω [b]	$n_{2\omega}$	l_c [c] (μm)	$\chi^{(2)}$ (pm/V)
$x = 5$	397.3	230	270	2.18	2.06	2.83	0.35
$x = 10$	398.5	230	290	2.23	2.12	2.53	2.17
$x = 15$	377.2	190	250	2.26	2.15	2.35	3.99
$x = 20$	302.9	170	230	2.29	2.16	2.15	3.32

[a] T_g is the glass transition temperature, T_o is the minimum poling temperature at which SHG can be detected, T_{opt} is the optimal poling temperature

[b] n_ω and $n_{2\omega}$ are the refractive indices at the wavelength of 1,064 and 532 nm, respectively

[c] l_c is the calculated coherent length

0.05 mol/L concentration KOH solution. Figure 7 shows the relative SH intensity of thermally poled $70GeS_2{\cdot}15Ga_2S_3{\cdot}15PbI_2$ glass sample of which the anode side surface portion has been removed by polishing to different depths. It is seen that SH intensity is gradually weakened as one proceeds to the inside of the sample and after an etching of a 10 μm thickness from the anodic face, the SH intensity decreases to about 8% of its original level. But the signal to noise ratio remained significantly higher than in a no poled $70GeS_2{\cdot}15Ga_2S_3{\cdot}15PbI_2$ glass. Then, we polished the cathodic face of the sample, whereas the SH intensity did not significantly change with the thickness of the sample.

One important feature should be emphasized for the thermally poled chalcohalide glass is the stability of second-order non-linearity induced in the glass. The inset in Fig. 7 shows the variation of SH intensity with time at room temperature after the poling. The glasses were kept in dark during each measurement. The measured sample does not manifest a decrease in SH intensity within the first 3 days, and after that, a decay of SH intensity is observed, but more than 80% of the initial value of SH intensity was obtained even 1 month after the poling.

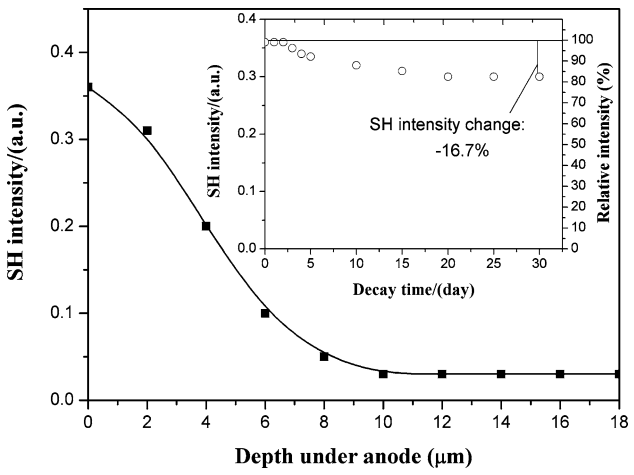

Fig. 7 Evolution of the SH intensity for the $70GeS_2{\cdot}15Ga_2S_3{\cdot}15PbI_2$ glass as a function of the depth under the anode-side surface after 0.05 mol/L KOH solution etching operations. The inset shows the decay of the SH intensity for $70GeS_2{\cdot}15Ga_2S_3{\cdot}15PbI_2$ glass after the poling

Discussion

Several explanations about the origin of the second-order non-linearity in bulk glass have been put forward. One is that the external excitation field results in the emergence of a spatially modulated local direct-current electric field, E_{dc}, which, via a third-order susceptibility $\chi^{(3)}$ (finite in isotropic materials), induces a spatially modulated second-order non-linearity as following expression [15]:

$$\chi^{(2)} \propto 3\chi^{(3)}E_{dc}. \quad (1)$$

It is known that the implementation of the field E_{dc} is related to the migration of mobile ions (for instance, Na^+ in the case of silica glasses) towards the cathode surface of the poled material. In GeS_2–Ga_2S_3–PbI_2 chalcohalide glass, considering the large atomic weight and volume of the cations, migration is hard to carry out. On the other hand, the fact that SH intensity decreases just below the glass transition temperature cannot be explained under the above-described model which assumes the mobile cations.

In fact, chalcogenide and chalcohalide glasses always contain large amounts of defects. As for GeS_2–Ga_2S_3–PbI_2 glass, large amounts of Ge–S, Ga–S, Ge–I, Ga–I and Pb–I electric dipoles are present in the structure. So an induced dipole orientation model is proposed. We suppose that dipoles are induced and oriented in the process of thermal poling.

According to dipole orientation model, second-order non-linearity can be created through following formula [16]:

$$\chi^{(2)} \propto Nf_{2\omega}f_\omega^2\beta\langle\cos^3\theta\rangle \quad (2)$$

where N is the number of effective dipoles, i.e. the reoriented dipoles, β is the second-order polarizability for each dipole, f is the local field factor, and θ is the angle between the dipole and the direction of external electric field.

The orientation of dipoles is mainly affected by three factors. First, restrain of glass network to dipoles, namely, the barrier energy of glass. Second, external activation energy for movement of dipoles. Third, thermal fluctuation of dipoles. Generally, the defects in glass are in different energy states, so the number of dipoles, which have enough activation energy to orientate is different. For each sample, we consider that the dipole number in it is fixed but the effective dipole number N is not fixed, and when the poling voltage and time are constant, N is determined by poling temperature.

Moreover, according to the etching experiment, the thickness of the non-linear layer at the anodic face is less than 10 μm, indicating that the orientation of dipoles is just limited in this thin layer beneath the glass surface.

The results in Fig. 4 can be explained by above dipole model. We can find out that there exists a minimum poling temperature T_o at which SHG can be detected for each glass, which is 190 °C for $x = 15$ for example. At room temperature without external dc voltage, all dipoles are fettered by network and just dispersed randomly. When the temperature is higher than T_o, some dipoles will obtain enough activation energy to overcome the restrain of glass network, and the symmetry center in the glass is broken down, therefore SH signals can be observed easily. Here, higher poling temperature can achieve higher number of the effective dipoles thus induce larger SH intensity. When the temperature is above T_{opt} and below T_g, the orientation of induced dipoles turns to disorder due to thermal fluctuation and structure relaxation around the glass transition temperature [3, 17], therefore SH signals decay.

The results in Fig. 5 are related to the structural variation. Investigations of Raman scattering spectra for $(100 - 2x)GeS_2{\cdot}xGa_2S_3{\cdot}xPbI_2$ glass system showed that as the Ga_2S_3 and PbI_2 additions, the amount of original basic structural units [GeS_4] tetrahedra decrease whereas mixed-anion [S_3GeI], [S_3GaI] and [S_2GeI_2] tetrahedra are formed gradually [18]. Additionally, in the component with high amount of PbI_2, some [PbI_n] structural units appear. Because of the chain-terminating function of iodine, the structural evolution will result in the decrease of structure rigidity, in other words, the increase of structure flexibility. In $(100 - 2x)GeS_2{\cdot}xGa_2S_3{\cdot}xPbI_2$ series glasses, with increasing of x, the glass transition temperature T_g decreases, which is a reflection of the increase of structure flexibility. The tight relations between characteristic temperature of poling (T_o, T_{opt}) and T_g can be explained as follows. For the composition with a larger mole percent x, it has a relatively lower T_g, and as poling temperature increases, rapid structural flexibility can be achieved thus makes barrier energy lower. This leads to more dipoles can break the tie of glass network and contribute to $\chi^{(2)}$.

In this investigated glass series, with increasing x, second-order susceptibility $\chi^{(2)}$ shows an increase first and then decrease. This can be explained by the accompanying changes in their structure. At first, with the increasing Ga_2S_3 and PbI_2 contents, structure flexibility is improved as we mentioned above, leading to enhancement of amount of the effective dipoles N in Eq. 2; meanwhile, because of the high polarization of Pb and I atoms, the second-order polarizability for each dipole can be remarkably improved, i.e., the value of β in Eq. 2 is increased. So we can understand that the addition of Ga_2S_3 and PbI_2 have contribution to improve the $\chi^{(2)}$. On the contrary, more structure flexibility means the dipoles will vibrate more vigorously, which causes the inner frozen-in process hard to be realized [3]. This leads to a reduction in reorientation of dipoles and decrease of $\chi^{(2)}$. The above two aspects have contradictive effects. When $5 \leq x \leq 15$, the first aspect has more profound influence, and when $x = 20$, the second aspect is dominant. The second aspect is considered responsible for the decay of SH intensity in the poled chalcohalide glasses.

Conclusion

The second-order non-linearity of the $(100 - 2x)GeS_2{\cdot}x$-$Ga_2S_3{\cdot}xPbI_2$ ($x = 5$, 10, 15, and 20) chalcohalide glasses was examined by utilizing Maker fringe measurements. It was found that there exist a minimum poling temperature T_o at which SHG can be detected and an optimal poling temperature T_{opt} for each sample with different compositions. Moreover, the optimal poling temperature of each composition is generally ~100 °C below the glass transition temperature T_g. At their own optimal poling temperature, the samples had different second-order susceptibility $\chi^{(2)}$ with the same applied voltage and poling duration and a maximum of $\chi^{(2)}$ as great as 4 pm/V was obtained at $x = 15$. A dipole reorientation model and structural relaxation causing by Ga_2S_3 and PbI_2 were proposed to explain the dependences of poling temperature on SH intensity for each composition and the presence of the maximum $\chi^{(2)}$ in this system.

Acknowledgment This work was partially funded by the National Natural Science Foundation of China (No. 50125205), the Opening Fund of Key Laboratory of Silicate Materials Science and Engineering (Wuhan University of Technology) Ministry of Education (No. SYSJJ2004-14).

References

1. Alley TG, Brueck SRJ (1998) Opt Lett 23:1170
2. Kudlinski A, Martinelli G, Quiquempois Y (2005) Opt Lett 30:1039
3. Tanaka K, Narazaki A, Hirao K, Soga N (1996) J Appl Phys 79:3798
4. Nasu H, Kurachi K, Mito A, Okamoto H, Matsuoka J, Kamiya K (1995) J Non-Cryst Solids 181:83
5. Miyata M, Nasu H, Mito A, Ohta Y, Kamiya K (1998) J Ceram Soc Jpn 106:135
6. Jain RK, Lind RC (1983) J Opt Soc Am 73:647
7. Liu QM, Zhao XJ, Gan FX (2000) Acta Phys Sin-CH ED 49:1726
8. Liu QM, Gan FX, Zhao XJ, Tanaka K, Narazaki A, Hirao K (2001) Opt Lett 26:1347
9. Qiu JR, Si J, Hirao K (2001) Opt Lett 26:914
10. Guignard M, Nazabal V, Troles J, Smektala F, Zeghlache H, Quiquempois Y, Kudlinski A, Martinelli G (2005) Opt Express 13:789
11. Guignard M, Nazabal V, Smektala F, Zeghlache H, Kudlinski A, Quiquempois Y, Martinelli G (2006) Opt Express 14:1524
12. Nakane Y, Nasu H, Heo J, Hashimoto T, Kamiya K (2005) J Ceram Soc Jpn 113:728
13. Guo HT, Zhai YB, Tao HZ, Gong YQ, Zhao XJ (2007) Mater Res Bull 42:1111
14. Dong GP, Tao HZ, Xiao XD, Lin CG, Zhao XJ, Mao S (2007) J Phys Chem Solids 68:158
15. Alley TG, Brueck SRJ, Myers RA (1998) J Non-Cryst Solids 242:165
16. Pretre Ph, Wu LM, Knoesen A (1998) J Opt Soc Am B 15:359
17. Takebe H, Kazansky PG, St Russell PJ, Morinaga K (1996) Opt Lett 21:468
18. Guo HT, Tao HZ, Zhai YB, Mao S, Zhao XJ (in press) Spectrochim Acta Part A: Mol Biomol Spectrosc doi: 10.1016/ j. saa. 2006. 10. 023